# 3D Reconstruction Optimization Using Imagery Captured By Unmanned Aerial Vehicles

**Abby Bassie, Sean Meacham, David Young, Gray Turnage, and Robert J. Moorhead**

Geosystems Research Institute, Mississippi State University, Mississippi State, MS 39762-9627

Geosystems Research Institute Report 5068

March 2016

MISSISSIPPI STATE UNIVERSITY

GRI

# 3D Reconstruction Optimization Using Imagery Captured By Unmanned Aerial Vehicles

**Abby Bassie, Sean Meacham, David Young, Gray Turnage, and Robert J. Moorhead**

Geosystems Research Institute, Mississippi State University, Mississippi State, MS 39762-9627

## Introduction

Traditionally, piloted aircraft and satellites have been the primary platforms for obtaining remote images. While they have obtained satisfactory imagery on a regional and global scale, these platforms have struggled to provide adequate spatial and temporal resolutions for data acquisition at a local scale (Torres-Sánchez et al. 2013). Unmanned aerial vehicles (UAV's) are playing an increasingly important role in remote imagery acquisition. Because these vehicles can fly at low altitudes, UAV's can collect ultra-high spatial resolution imagery and can observe small individual plants and patches (Xiang and Tian 2011).

One way that UAV imagery is used to differentiate between small objects of similar size is through three-dimensional (3-D) reconstruction. When a collection of images is taken over a test area, sorting algorithms compare pixels between similar images. As matching pixels are found in multiple images, these pixels are inserted into a three-dimensional point cloud. By correctly scaling these point clouds, accurate portrayals of objects can be digitally recreated *in silica*. Objects within these 3-D reconstructions can then be dimensionally measured. This technique is rising in popularity as a surveying tool, thus it is vitally important that researchers understand how to optimize the performance of UAV's and their associated camera payloads for 3-D reconstruction.

**Methods**

In this study, a Nikon RGB camera with a 10 mm lens was attached to a Precision Hawk Lancaster (version 4). A series of six flights were executed over a test plot at the R.R. Foil Plant Research Center (North Farm) at Mississippi State University (Figure 1) **using no ground control points** to simulate conditions in an inaccessible area. This test plot encompassed an area of 8.86 ha (21.89 ac) and contained nine predetermined reference objects (Figure 2). A few dimensions of these reference objects were measured using a tape measure prior to UAV flights. The first flight was conducted at an altitude of 45.72 m (150 ft.), and subsequent flight altitudes were increased by increments of 15.24 m (50 ft.) per flight. Flight plans were developed to provide 70% (frontal and lateral) overlap between images. Overlap greater than 70% can cause triggering issues in the shutter mechanism of the Nikon payload. After obtaining data from each flight, the images were processed using AgiSoft PhotoScan, a stand-alone software product that uses photogrammetry to create 3-D point clouds from digital images. Point clouds from each flight scenario were then exported from AgiSoft as '.ply' files and were imported into MeshLab, an open-sourced image processing software package.

MeshLab was utilized for point cloud analysis in this study because the software contains a readily accessible measuring tool. In order to use this tool, a known dimension of an object in the point cloud must be used to set the point cloud's scale. In each of the flight scenarios, the width of Reference Object 1 (x-direction) was used to set the scale of the point cloud for MeshLab measurement. The other known dimensions of the reference objects were used to analyze the accuracy of MeshLab measurements (Table 1).

After using Reference Object 1 to set the scale of the point cloud, MeshLab's measuring tool was used to measure dimensions of the reference objects. These measurements were then

compared to the actual dimensions of the reference objects. These changes are recorded as Δx, Δy, and Δz in Appendix A. The Δx, Δy, and Δz values at each altitude were then averaged to show average change in each coordinate direction for each of the six flight scenarios (Table 2).

**Results**

While over 900 photos were required to obtain 70% overlap in the 45.72 m (150 ft.) scenario, only 156 photos were required to obtain the same amount of image overlap at 121.92 m (400 ft.). Additionally, high altitude flights significantly reduced AgiSoft computation time in comparison to lower altitude flights. Processing for the 45.72 m flight took around 30 hours, while the processing time for the 121.92 m flight was only approximately 5 hours (Table 2).

While flying at higher altitudes reduced processing time and energy costs in comparison to flights performed at lower altitudes (Table 2), there was a substantial loss in spatial resolution at high altitudes. Only two measurements could be made in the point cloud generated at 121.92 m. Most of the reference objects in the point cloud generated from images at this altitude were too pixelated to clearly identify and measure. The reference objects in the point cloud generated from an altitude of 76.2 m (250 ft.), however, were much easier to identify and measure. In this flight scenario, seven of the nine reference objects had measurable dimensions (Appendix A). When the point clouds from the 60.96 m (200 ft.) and 45.72 m (150 ft.) flights were imported into MeshLab, the software crashed. This commonly happens when the size of the data set exceeds MeshLab's computational capabilities. In the future, images from the 60.96 m and 45.72 m flights will be processed using a reduced number of images.

**Discussion and Conclusions**

While the 121.92 m (400 ft.) flight yielded the smallest average Δx and Δz, the spatial resolution of point clouds generated at this altitude must be taken into account. Spatial resolution

at this altitude was so poor that only two measurements could be obtained from the reference objects. This problem was solved at the lower altitude flights, as increased spatial resolution improved the number of measurable reference objects (Appendix A). This study does suggest that the lower the altitude, the higher the spatial resolution of point clouds; however, MeshLab seems to be unable to handle datasets larger than approximately 360 – 400 images. Additionally, because the operator manually makes measurements on point clouds in MeshLab, a certain amount of operator error will always factor into the accuracy of measurements made by this tool. Refinement of the point cloud scale and precise measurements help ensure that operator error is minimal.

In three of the scenarios flown in this study, MeshLab had the capability to measure object dimensions from 50.8 to 76.2 cm (20 – 30 inches) with greater than 93% accuracy (Appendix A). The largest average deviation in any flight scenario from actual measurements was 14.773 cm (5.816 in.). These results are satisfactory in a wide variety of research applications focused on differentiating objects using remote imagery.

It is possible that MeshLab measurements could be further optimized by investigating variables outside the scope of this study. MeshLab's measuring tool may be more accurate when measuring objects at a larger scale or when used with point clouds constructed with different image overlap settings. Because these refinements are important to optimization of UAV's as a platform for 3-D reconstruction, research investigations focused on these topics are currently underway.

## Literature Cited

Torres-Sánchez, J., F. López-Granados, A.I. De Castro, J.M. Peña-Barragán. 2013. Configuration and Specifications of an Unmanned Aerial Vehicle (UAV) for Early Site Specific Weed Management. PLoS ONE 8(3): e58210. doi:10.1371/journal.pone.0058210. Access March 2016.

Xiang, H. and L. Tian. 2011. Development of a low-cost agricultural remote sensing system based on an autonomous unmanned aerial vehicle (UAV). *Biosyst Eng* 108(2): 174–190. http://www.sciencedirect.com/science/article/pii/S1537511010002436. Access March 2016.

## Tables and Figures

**Table 1.** Reference objects and their actual dimensions

| Reference Object # | x (cm) | y (cm) | z (cm) |
|---|---|---|---|
| **1** | 149.86 | - | 69.85 |
| **2** | 78.74 | - | 54.61 |
| **3** | 64.77 | - | 16.7132 |
| **4** | 78.74 | - | - |
| **5** | 57.4675 | - | - |
| **6** | 66.04 | 66.04 | - |
| **7** | 97.155 | 78.74 | 80.01 |
| **8** | 78.74 | - | - |
| **9** | - | - | 38.1 |

**also used cap of Reference Object 1. x cap (cm) = 66.04

**Table 2.** Average change from actual measurements for each flight scenario.

| Altitude (m) | Δx (cm) | Δy (cm) | Δz (cm) | Area (Ha) | Image Count | Processing Time (hours) |
|---|---|---|---|---|---|---|
| **400** | 0.596 | N/A | 0.625 | 8.86 | 156 | 5 |
| **350** | 2 | -0.872 | -5.816 | 8.86 | 190 | 7 |
| **300** | 3.916 | 0.851 | -0.733 | 8.86 | 225 | 10 |
| **250** | -1.191 | -3.384 | 1.971 | 8.86 | 360 | 13 |
| **200** | N/A | N/A | N/A | 8.86 | 533 | 20 |
| **150** | N/A | N/A | N/A | 8.86 | 927 | 30 |

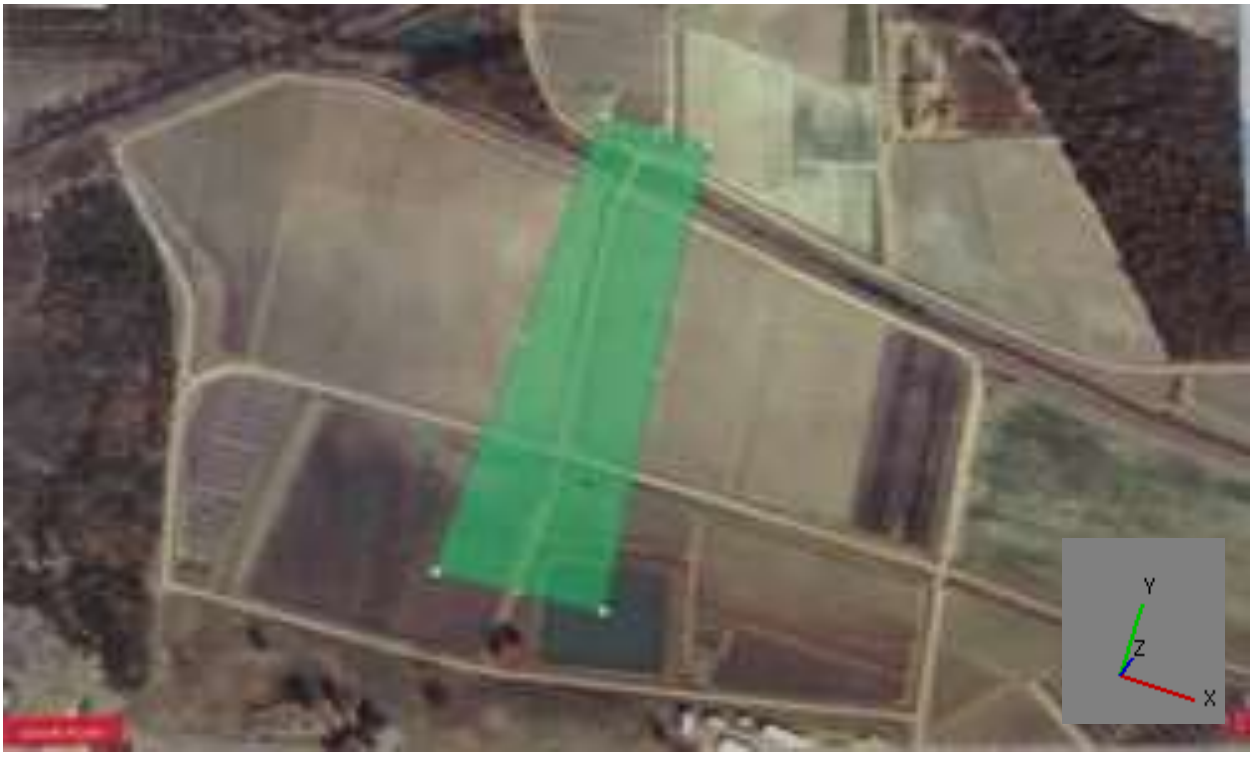


**Figure 1.** Flight plan over the R.R. Foil Plant Research Center at Mississippi State University.


**Figure 2.** Reference objects at the R.R. Foil Plant Research Center at Mississippi State University.

## Appendices

Appendix A. This appendix shows the deviation of MeshLab measurements from actual measurements of reference object dimensions. Values are shown (+) when MeshLab measurements were larger than the actual measurement and (-) when MeshLab measurements were less than the actual measurements. All values are given in cm. Any measurements that could not be performed in MeshLab are marked with "-- --"

| Reference Object # | Dimension | 150 | 200 | 250 | 300 | 350 | 400 |
|---|---|---|---|---|---|---|---|
| 1 | ΔX | -- -- | -- -- | -1.204 | +0.762 | -1.27 | +0.596 |
| | ΔY | -- -- | -- -- | -- -- | -- -- | -- -- | -- -- |
| | ΔZ | -- -- | -- -- | +4.422 | -- -- | -- -- | -- -- |
| 2 | ΔX | -- -- | -- -- | +0.338 | +2.91 | -3.973 | -- -- |
| | ΔY | -- -- | -- -- | -- -- | -- -- | -- -- | -- -- |
| | ΔZ | -- -- | -- -- | -0.016 | -- -- | -- -- | -- -- |
| 3 | ΔX | -- -- | -- -- | -0.686 | +4.62 | +2.16 | -- -- |
| | ΔY | -- -- | -- -- | -- -- | +1.97 | -- -- | -- -- |
| | ΔZ | -- -- | -- -- | -- -- | -- -- | -- -- | -- -- |
| 4 | ΔX | -- -- | -- -- | -1.185 | +7.612 | +11.48 | -- -- |
| | ΔY | -- -- | -- -- | -- -- | -- -- | -- -- | -- -- |
| | ΔZ | -- -- | -- -- | -- -- | -- -- | -- -- | -- -- |
| 5 | ΔX | -- -- | -- -- | -1.667 | +0.523 | +1.602 | -- -- |
| | ΔY | -- -- | -- -- | -- -- | -- -- | -- -- | -- -- |
| | ΔZ | -- -- | -- -- | -- -- | -- -- | -- -- | -- -- |
| 6 | ΔX | -- -- | -- -- | -- -- | -- -- | -- -- | -- -- |
| | ΔY | -- -- | -- -- | -3.384 | -0.166 | -0.872 | -- -- |
| | ΔZ | -- -- | -- -- | -- -- | -- -- | -- -- | -- -- |
| 7 | ΔX | -- -- | -- -- | -2.391 | -- -- | -- -- | +0.625 |
| | ΔY | -- -- | -- -- | -- -- | +0.749 | -- -- | -- -- |
| | ΔZ | -- -- | -- -- | +1.508 | -0.733 | -5.816 | -- -- |
| 8 | ΔX | -- -- | -- -- | -- -- | -- -- | -- -- | -- -- |
| | ΔY | -- -- | -- -- | -- -- | -- -- | -- -- | -- -- |
| | ΔZ | -- -- | -- -- | -- -- | -- -- | -- -- | -- -- |
| 9 | ΔX | -- -- | -- -- | -- -- | -- -- | -- -- | -- -- |
| | ΔY | -- -- | -- -- | -- -- | -- -- | -- -- | -- -- |
| | ΔZ | -- -- | -- -- | -- -- | -- -- | -- -- | -- -- |